LA-UR-16-21613
Approved for public release; distribution is unlimited.

Title: Morphological Comparison of U3O8 Ore Concentrates from Canada Key Lake and Namibia Sources

Author(s): Schwartz, Daniel S.
Tandon, Lav
Martinez, Patrick Thomas

Intended for: Report

Issued: 2016-03-11

Morphological Comparison of U_3O_8 Ore Concentrates from Canada Key Lake and Namibia Sources

Daniel S. Schwartz, Lav Tandon, Patrick Martinez

Introduction

Uranium ore concentrates from two different sources were examined using scanning electron microscopy (SEM) and energy dispersive spectroscopy (EDS). The ore powders are referred to as Namibia (id. no. 90036, LIMS id. no. 18775) and Canada Key Lake (id. no. 90019, LIMS id. no. 18774). Earlier work identified the ores as the U_3O_8 phase of uranium oxide using x-ray diffraction (Figure 1).

Both sets of powders were in the form of dark brown to black powder fines. However, the Canada Key Lake concentrates contained larger chunks of material on the millimeter scale that were easily visible to the unaided eye.

The powders were mounted for SEM examination by hand dispersing a small amount onto conductive sticky tape. Two types of applicators were used and compared: a fine-tipped spatula and a foam-tipped applicator. The sticky tape was on a standard SEM “tee” mount, which was tapped to remove loose contamination before being inserted into the SEM.

General qualitative observations

At lower magnifications, distinct differences were observable between the two ore powder sets. The Namibia ore powder 1) was notably less regular in shape, 2) had a larger number of very small particles, and 3) appeared more friable than the Canada Key Lake (CKL) set. Figure 2 shows a typical set of particles from the Namibia set, which can be compared to a typical set from the CKL material in Figure 3. The CKL particle set clearly has a higher proportion of approximately elliptical particles. In addition, the

Namibia set was apparently more friable, as seen in Figure 2, which shows a numerous particles which have crumbled into smaller pieces. Large, friable particles were observed in both sets (examples are shown in Figure 4 and Figure 5).

The particles from both ore sets are highly porous. At high magnifications a clear difference between the sets can be seen. Figure 6 shows a close view of a large Namibia ore particle. A wide variety of pore sizes are visible, and the particle in Figure 6 has a highly friable appearance. The CKL particle surface shown in Figure 7 has a more regular appearance, with a well-defined pore morphology (~ 50 – 100 nm diameter). A high magnification view (Figure 8) of a small, < 10 µm diameter particle from the Namibia ore set shows the same general structure as that seen in the large particle in Figure 6. A high magnification view of a small CKL particle (Figure 9) shows that the CKL particles are composed of smaller, 100 – 200 nm diameter particles, which appear to be well bonded together.

Both powder sets contained a number of large particles (> 100 µm diameter), which can be difficult to statistically quantify using SEM, for several reasons. First, when we mount the particles on sticky tape we tap the SEM mount while in a sideways position to allow loosely affixed particles to fall off the mount. This action will preferentially dislodge larger particles. Secondly, the magnifications required to image particles in the 1 µm diameter range will necessarily preclude imaging particles in the > 100 µm range, as they will be larger than the SEM field of view. A third bias may arise from the use of a spatula to take subsamples from the larger powder samples, which is likely to favor collection of smaller particles. Larger particles will roll off a spatula preferentially compared to smaller particles. However, the number fraction of large particles within the population is clearly small, and most likely they represent < 0.1% of the total population. The MAMA software was used to measure two representative large particles from both sets and the analysis results are shown in Figure 10 (Namibia) and Figure 11 (CKL particle).

EDS proved to be of limited use for these particles, and was only able to detect U and O in both powder sets (Figure 12).

Comparison of Particle Application Methods

A variety of methods are available for applying particles to SEM stubs for morphological analysis. We compared three different methods: 1) sharp tipped spatulas, 2), sharp tipped spatulas onto obliquely tilted SEM stubs and 3) foam-tipped applicators. Different types of sharp tipped spatulas were employed, including commercial stainless steel spatulas, hand-sharpened plastic wedges, and pointed aluminum foil wedges. No real differences were observed between SEM stubs prepared using these different spatulas. Sharped tipped spatulas are easy to use, and work well in general for smaller particles (1 - 50 µm diameter). Wedge shaped spatulas in particular are suitable for making SEM mounts with sparse particle distributions, which are more suitable for morphological analysis than heavily loaded SEM mounts with overlapping particles. However, large, rounded particles preferentially roll off of spatulas as powder is transferred from the parent sample to the SEM stub, resulting in a statistical bias against large particles. For example, the CKL powder contained easily visible particles >500 µm diameter that were never captured using a wedge shaped spatula. The orientation of the SEM stub with respect to the particle spill path was varied, and the effect is visible in Figure 13 (Namibia ore above, CKL ore below). The particles adhere in a plume shaped configuration, which effectively spreads them out into a more sparse distribution. Tilting the SEM stub is therefore useful for spreading the particles out for morphological analysis and minimize overlapping particles. It should be noted that spreading the particles out into a plume does not appear to separate them by size. There is no obvious segregation by size as a function of position in the particle plume visible in Figure 13. Lint-free foam-tipped applicators were explored as means to capture large agglomerated particles, such as those present in the CKL ore concentrates. The applicators were gently touched to the parent powder then placed above a clean SEM stub and tapped, without allowing the applicator to touch the SEM stub. The resulting powder distribution is shown in Figure 14, and it can be seen that the large agglomerates are preserved. The agglomerates are loosely bound, and break apart on the SEM mount. It appears that the large 0.5 – 2.0 mm diameter agglomerates in the CKL powder set are primarily composed of smaller particles in the 10-50 µm diameter range.

Quantitative Morphological Analysis

The Morphological Analysis for Materials Attribution (MAMA) software package was used to measure particles from the CKL and Namibia powder sets. For completeness, the statistical parameters for all the

morphological parameters calculated by the software are listed in Table 1 (CKL ore, part 1), Table 2 (CKL ore, part 2), Table 3 (Namibia ore, part 1), and Table 4 (Namibia ore, part 2). We focused on the equivalent circular diameter (ECD) for further analysis, as this is a widely used and practical parameter for quantifying and comparing the size of particles. The statistical parameters for ECD are summarized in Table 5. The mean ECD for the Namibia set was less than that for the CKL ore (5.0 μm vs. 7.2 μm, respectively). This is a real, quantified discriminator between the two sets, as can be seen by examining the 95% confidence band, 0.32 for Namibia and 0.52 for CKL. At a 95% confidence level, the mean ECD for Namibia ore is in the range 4.68-5.32 μm and the mean for CKL is in the range 6.70-7.74 μm, so there is no overlap of the population means. The histograms for ECD distribution for both ores is shown in Figure 15, revealing that in addition to the different mean ECD, the CKL ore has a significantly higher fraction of larger (> 10μm) particles. The distributions show the expected log-normal shape (i.e. a sharp rise in value from 0, with a gradual fall to the minimum value after the peak), and the Namibia set is more sharply peaked. It is useful to examine the cumulative distribution (Figure 16), where is can be immediately seen that for all small ECDs, the Namibia ore has a significantly higher fraction in that size range. Choosing ECD = 10μm for example, it can be directly read from Figure 16 that the 94% of the Namibia set is below this size, compared to only 74% of the CKL set.

One notable difference between the powder sets was the presence of a significant number of elliptical particles in the CKL sets. This morphological observation can be quantified by calculating the ratio between the actual *measured* perimeter and the perimeter of the best-fit ellipse. This ratio will be close to 1 for particles which approximate an ellipse, and can be large for particles with wandering perimeters or shapes far from elliptical. Subjectively, a value < 1.3 for the “goodness of ellipse” (GoE) ratio represents a particle that would be described by most analysts as ellipsoidal. The GoE ratio was calculated for both powder sets, and a trend was apparent for the larger particles in the populations. The results are shown in a scatter plot, where the GoE ratio is plotted against the ECD (Figure 17). The scatter plot is restricted to larger particles with ECD > 10 μm, and it is clear that if we choose a cutoff of ~1.3 for the GoE, the scatter plot is dominated by points from the CKL particle set. Even more dramatically, at ECD > 20 μm there are *no* Namibia ore particles that are good ellipses with GoE < 1.3. Thus this methodology is a way to discriminate this morphological feature, i.e. how elliptical the particles are, in a quantitative way.

Acknowledgments

Thanks to W. Kinman and R. Steiner for supplying the U_3O_8 ore concentrates. Support for this study came from the Office of Nuclear Controls, NA-242, Confidence Building Measures Program, NNSA/DOE.

Figures

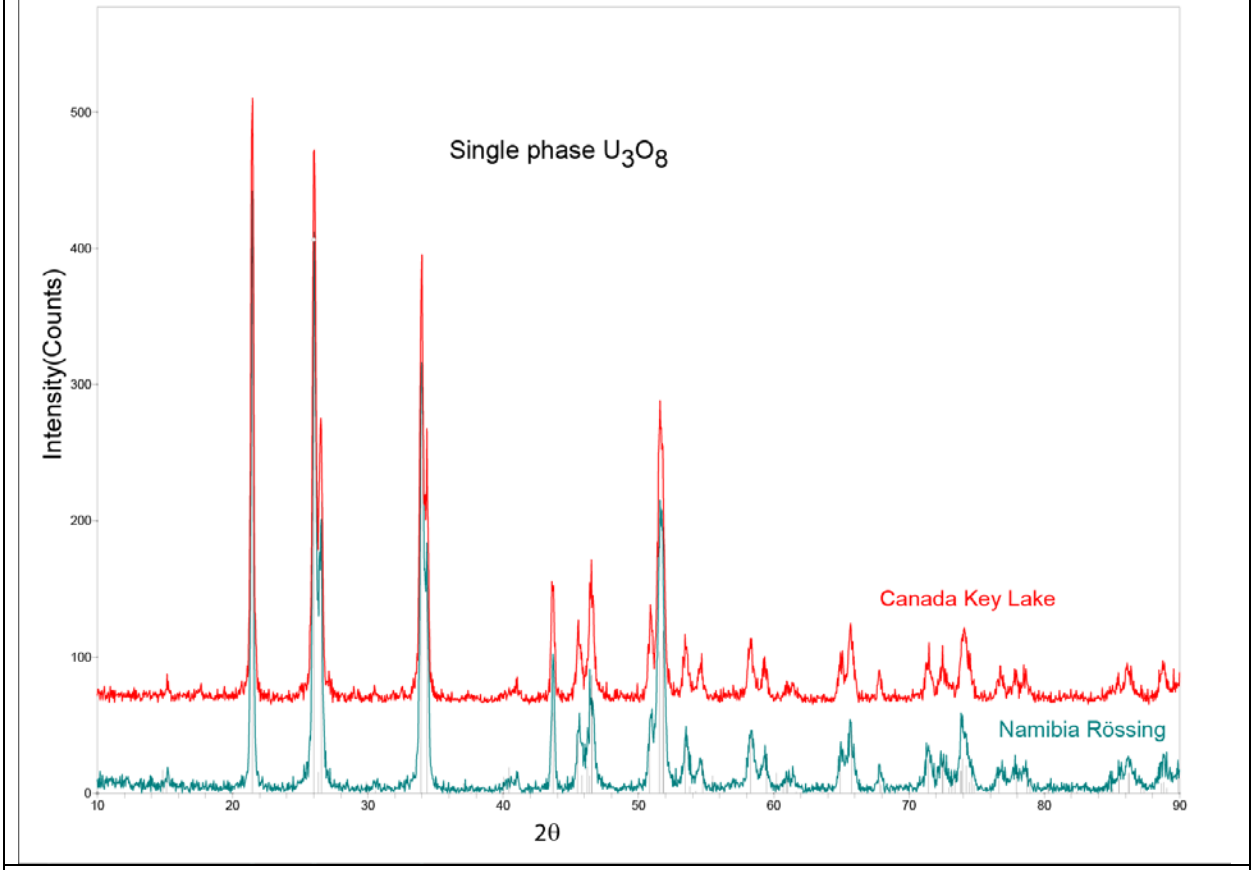

Figure 1. X-ray diffraction spectra from the two uranium ore concentrates used in this study. They are both U_3O_8 uranium oxides, and are indistinguishable using this analytical technique.

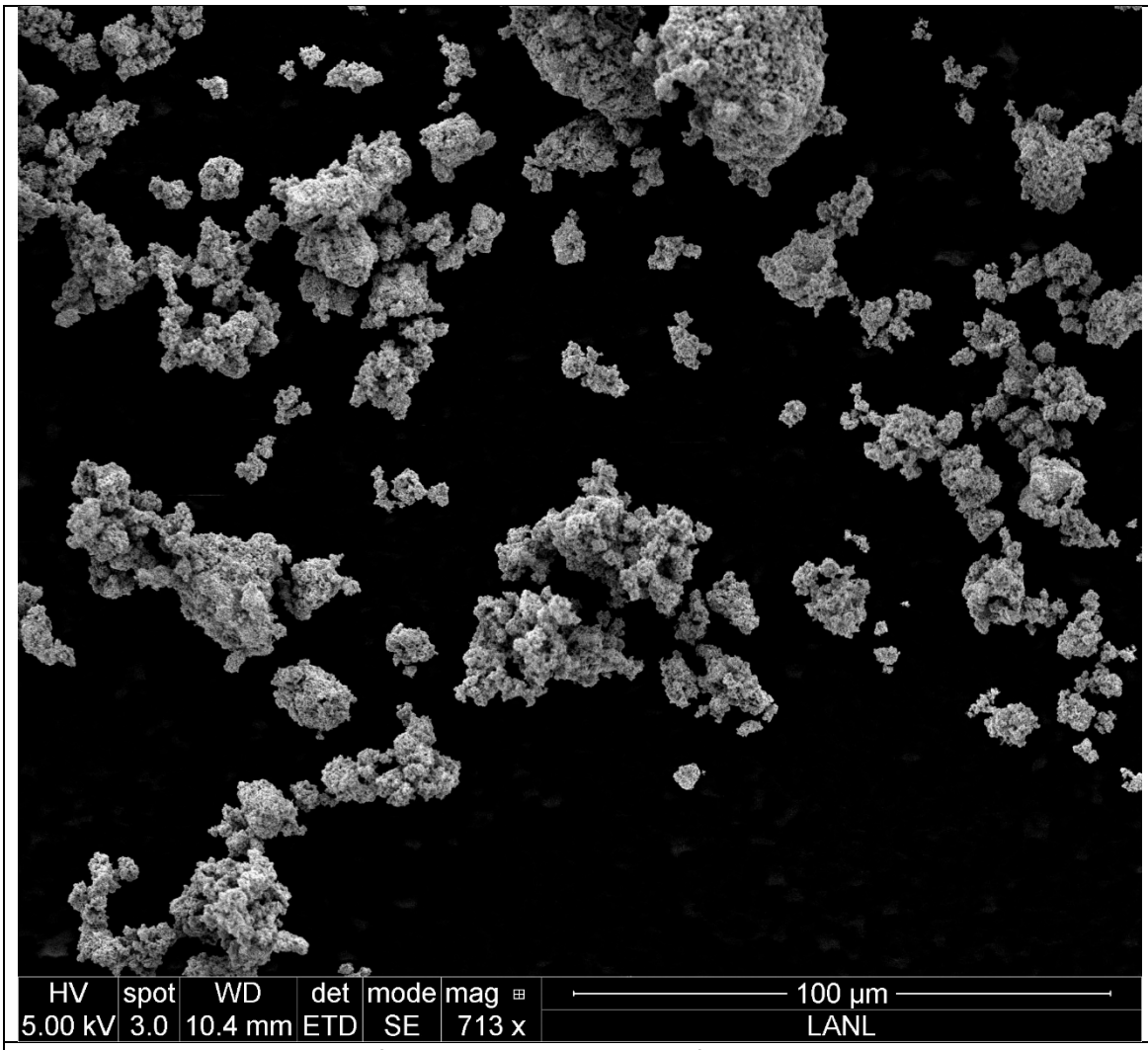

Figure 2. Typical appearance of Namibia ore at low magnification.

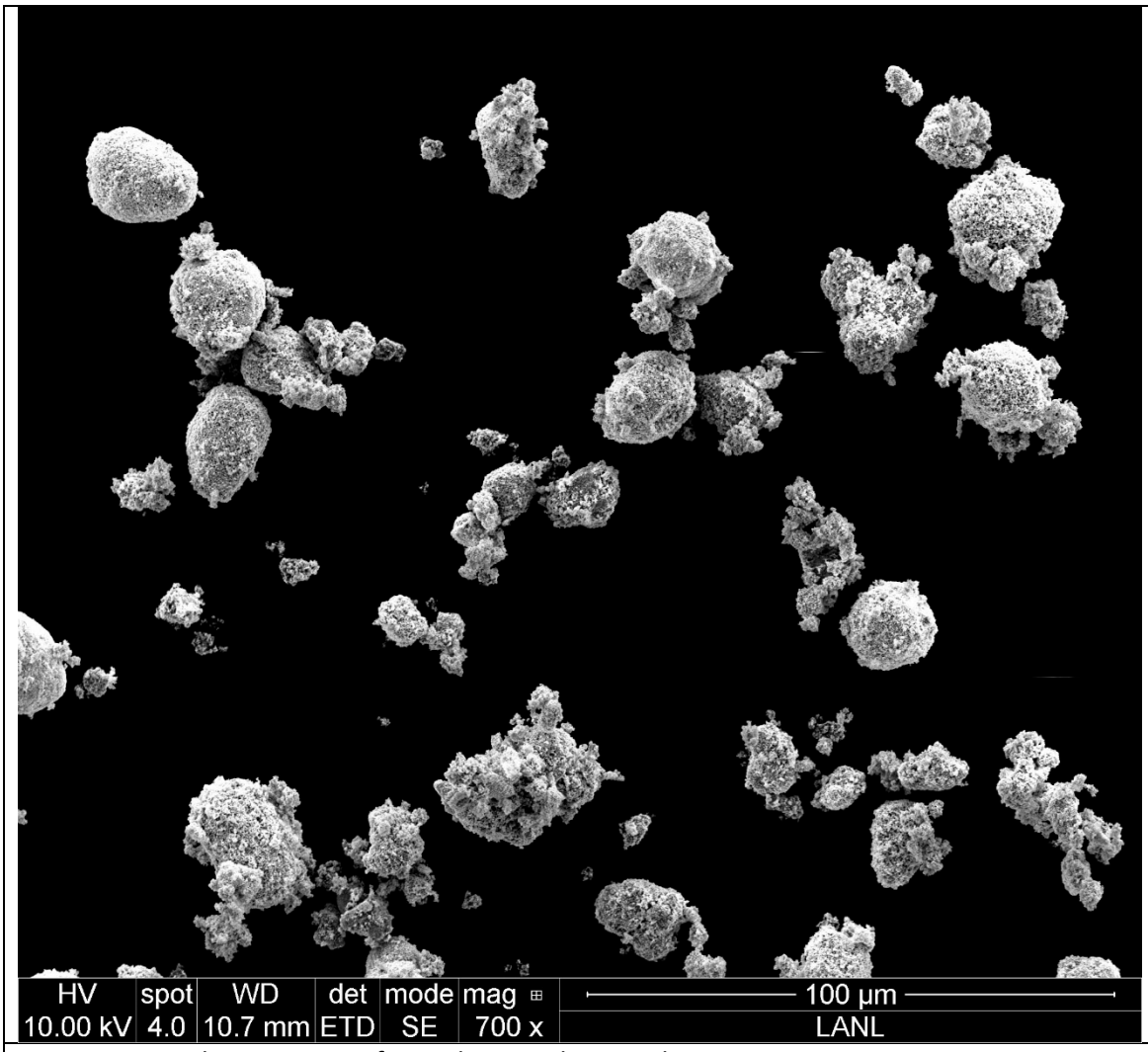

Figure 3. Typical appearance of Canada Key Lake particles.

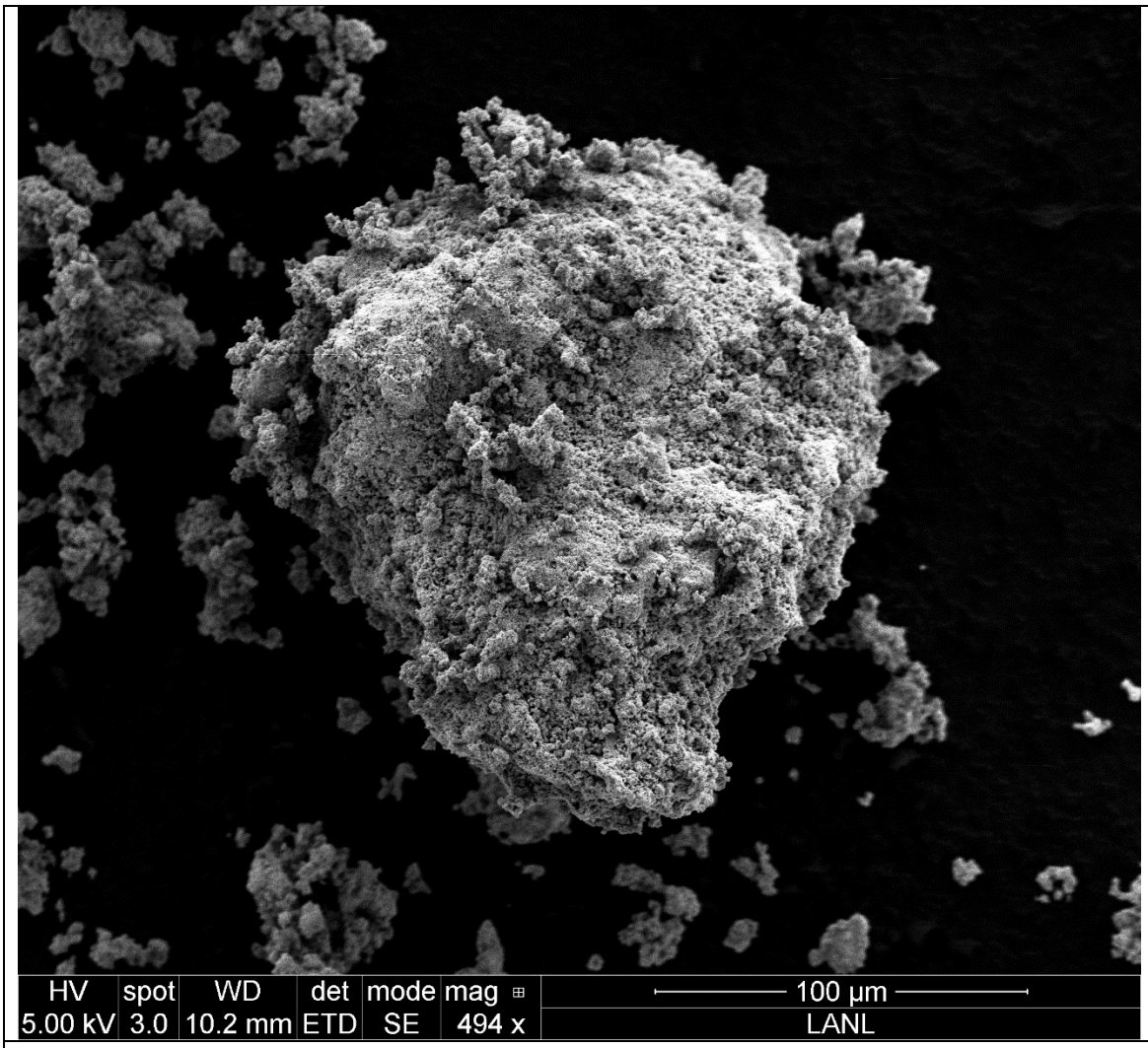

Figure 4. Typical large friable particle in the Namibia particle set.

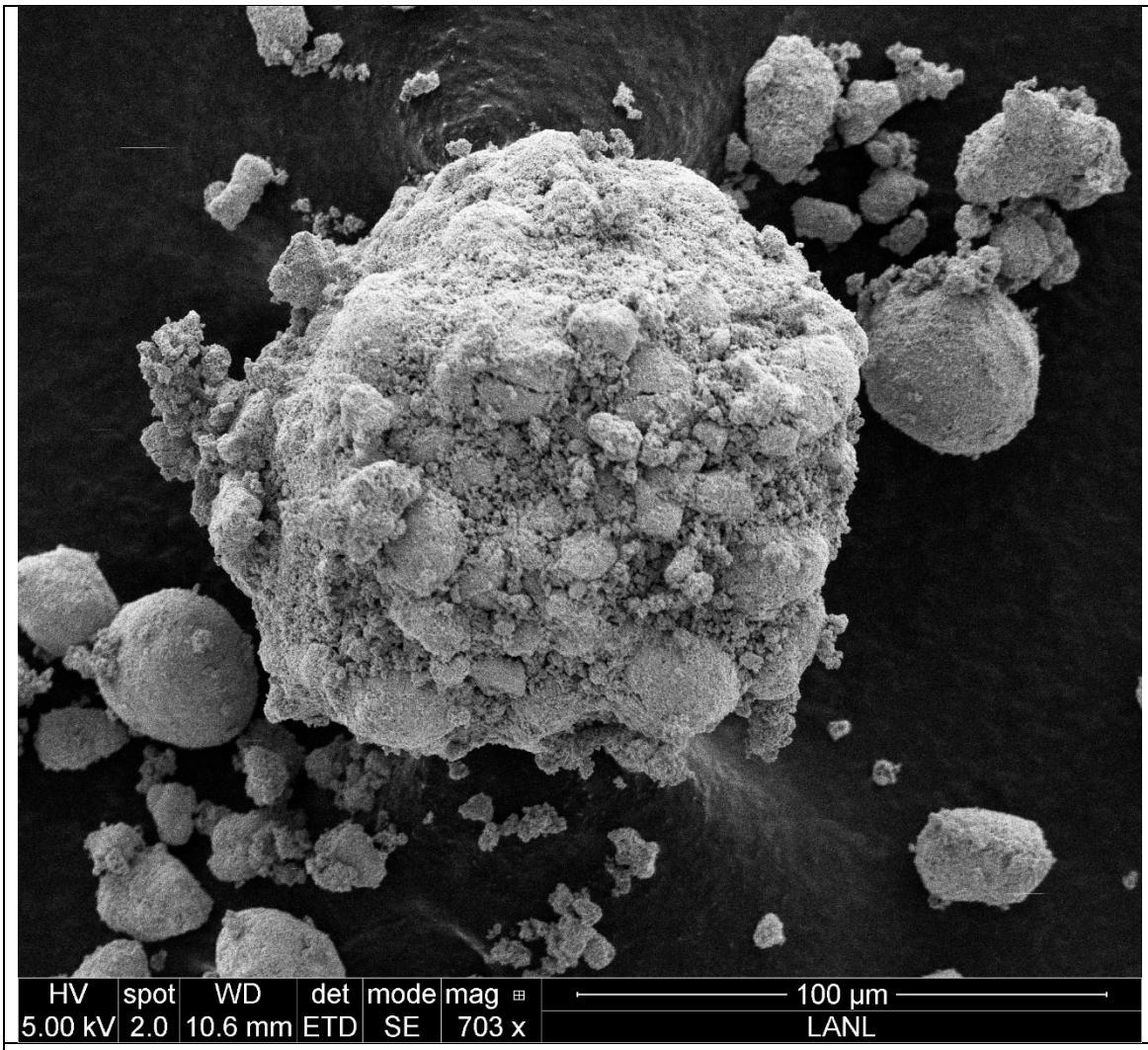

Figure 5. Large particle in CKL set, showing friable structure.

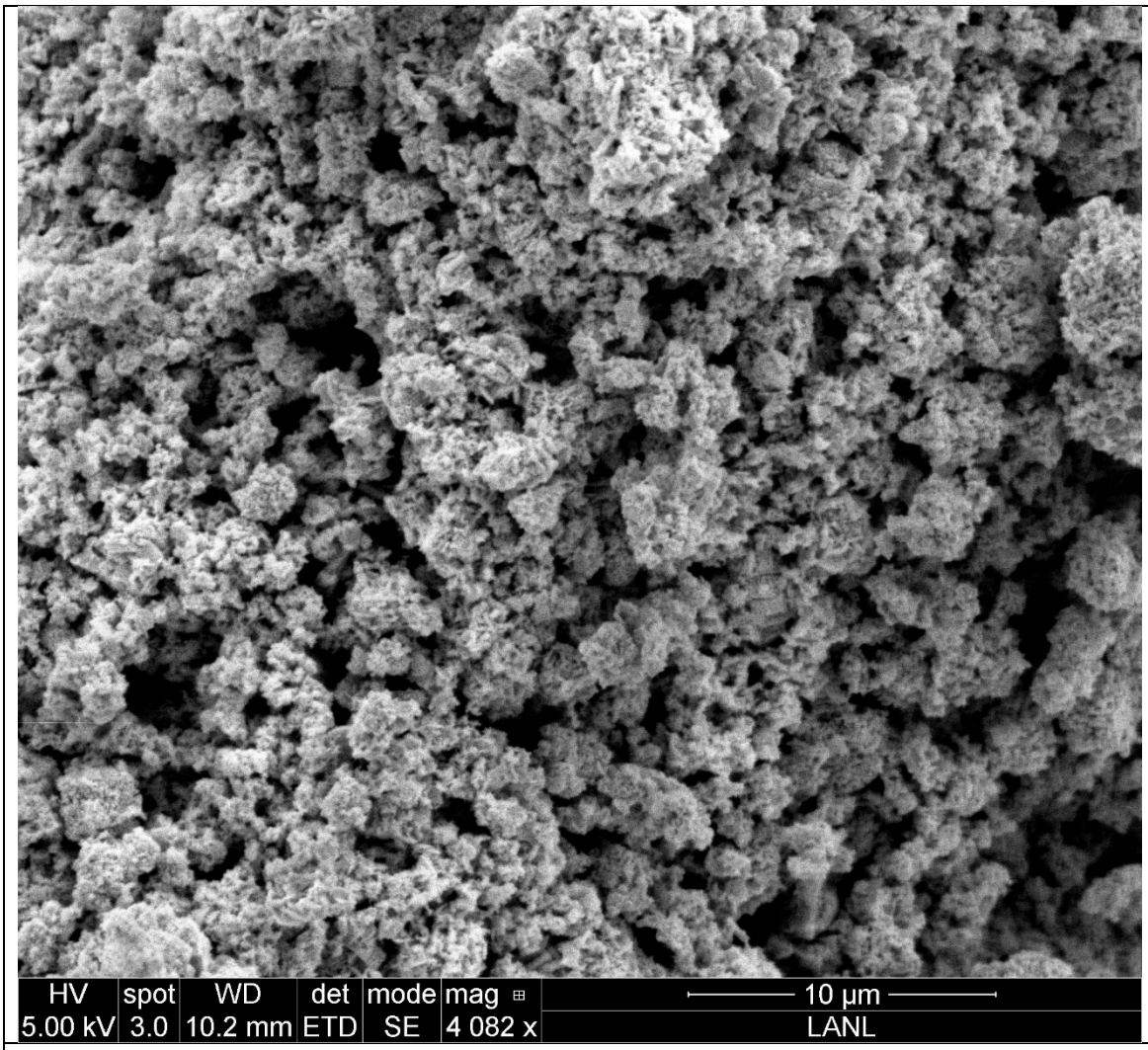

Figure 6. Close-up of the surface of a typical Namibia ore concentrate particle.

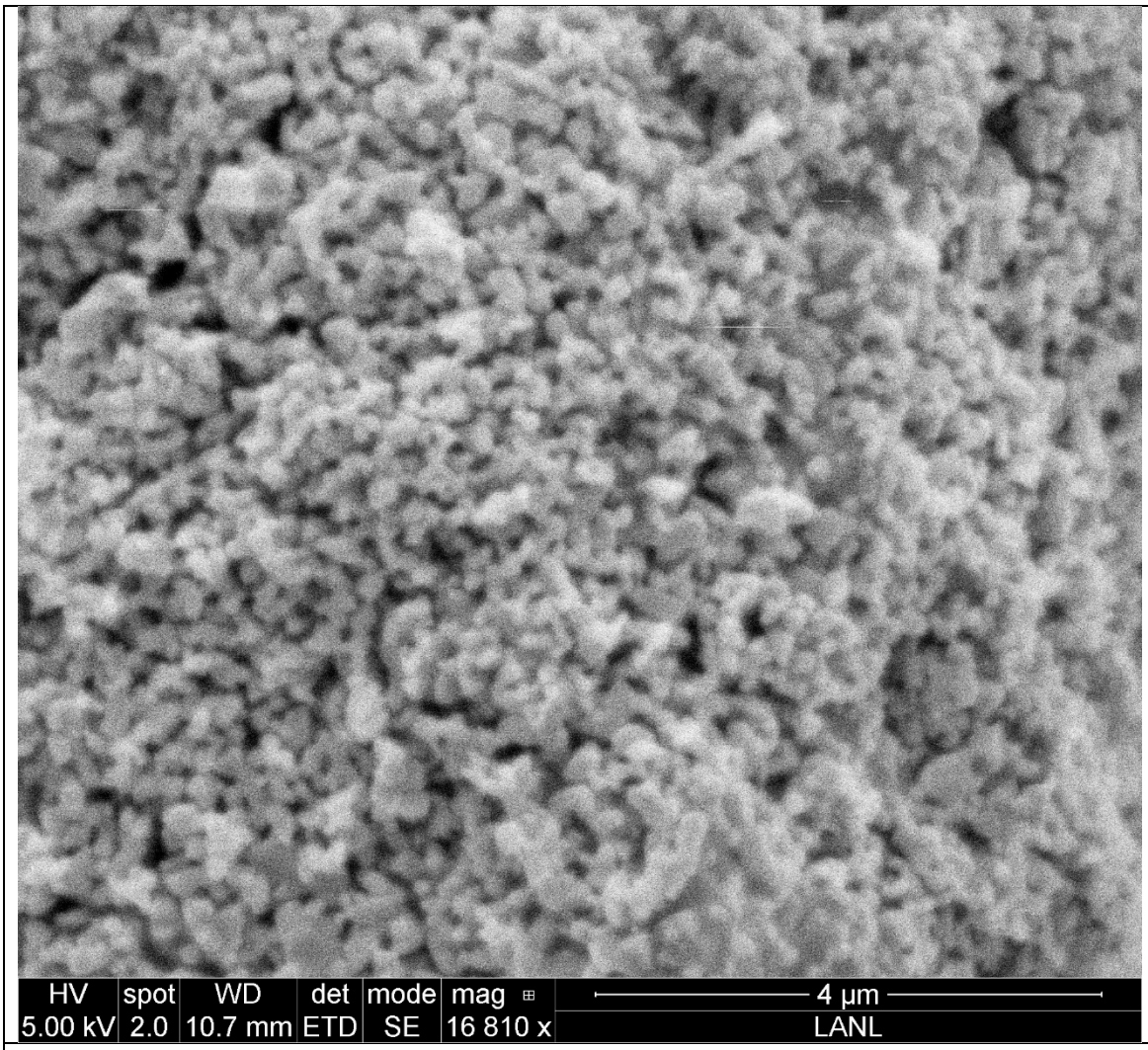

Figure 7. Close-up of porosity in a large CKL particle.

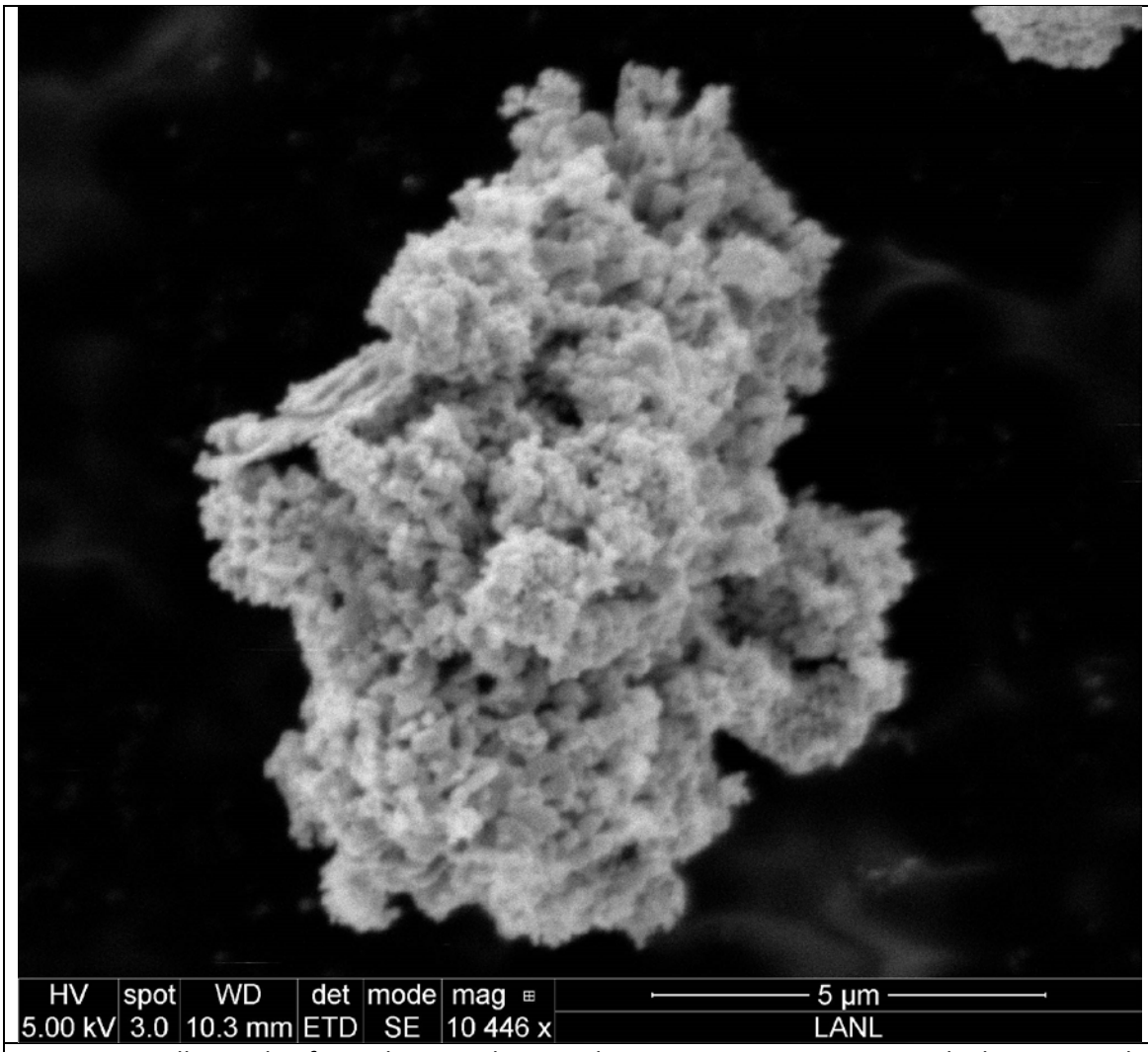

Figure 8. Small particle of Namibia ore, showing the same porous structure as the larger particles.

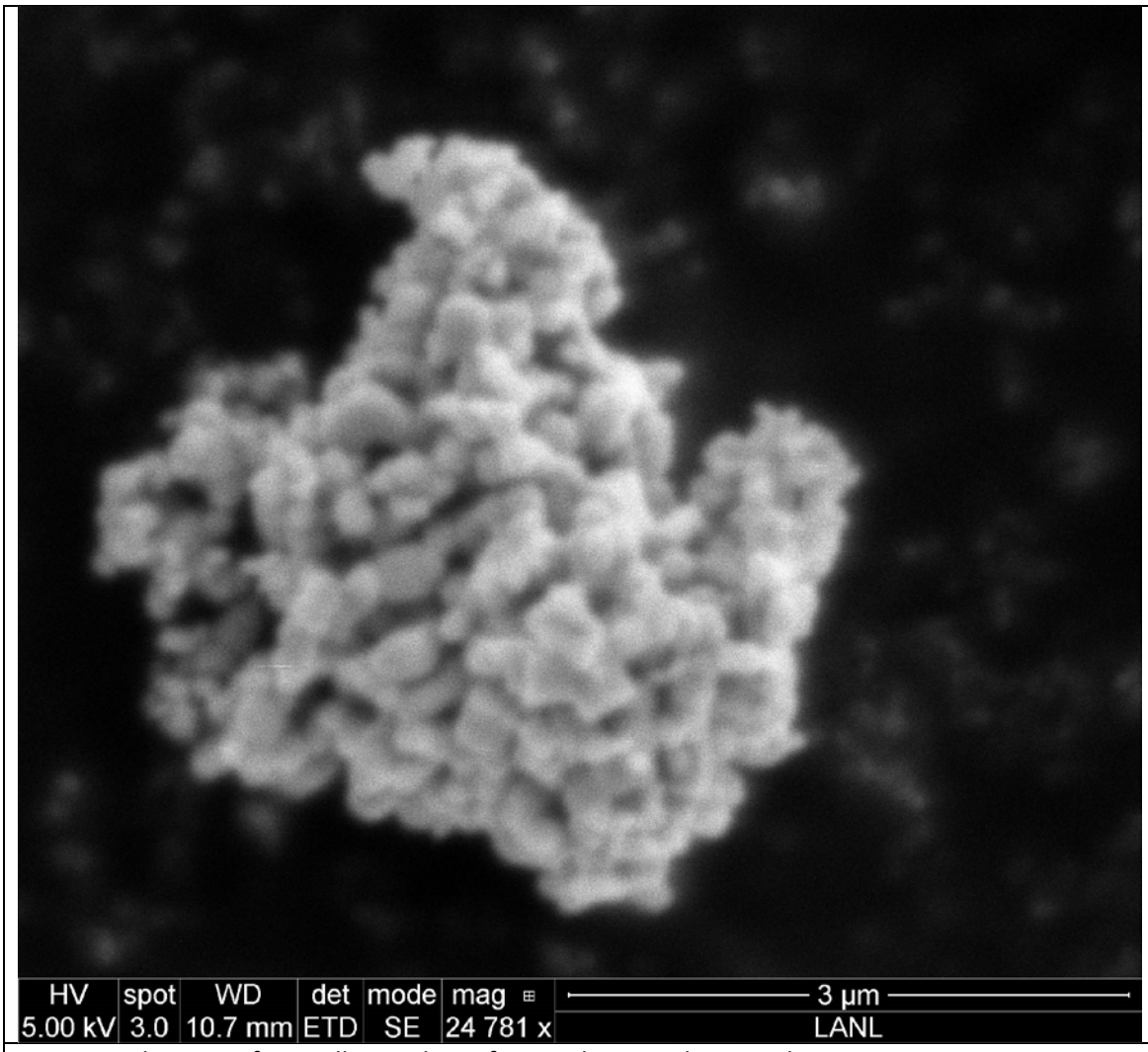

Figure 9. Close-up of a small particle surface in the Canada Key Lake ore.

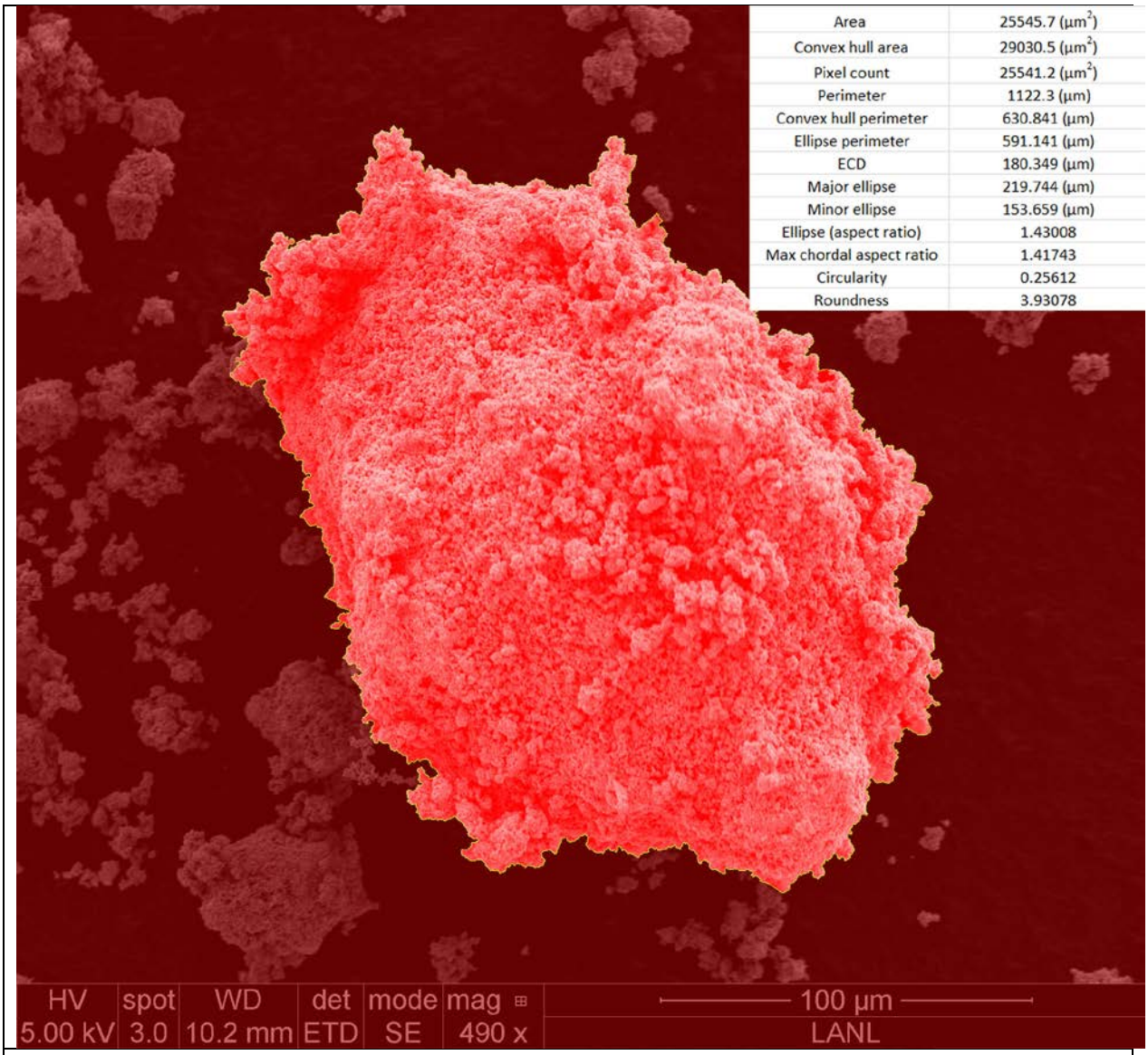

Figure 10. Large particle in Namibia ore with morphological parameters calculated using MAMA.

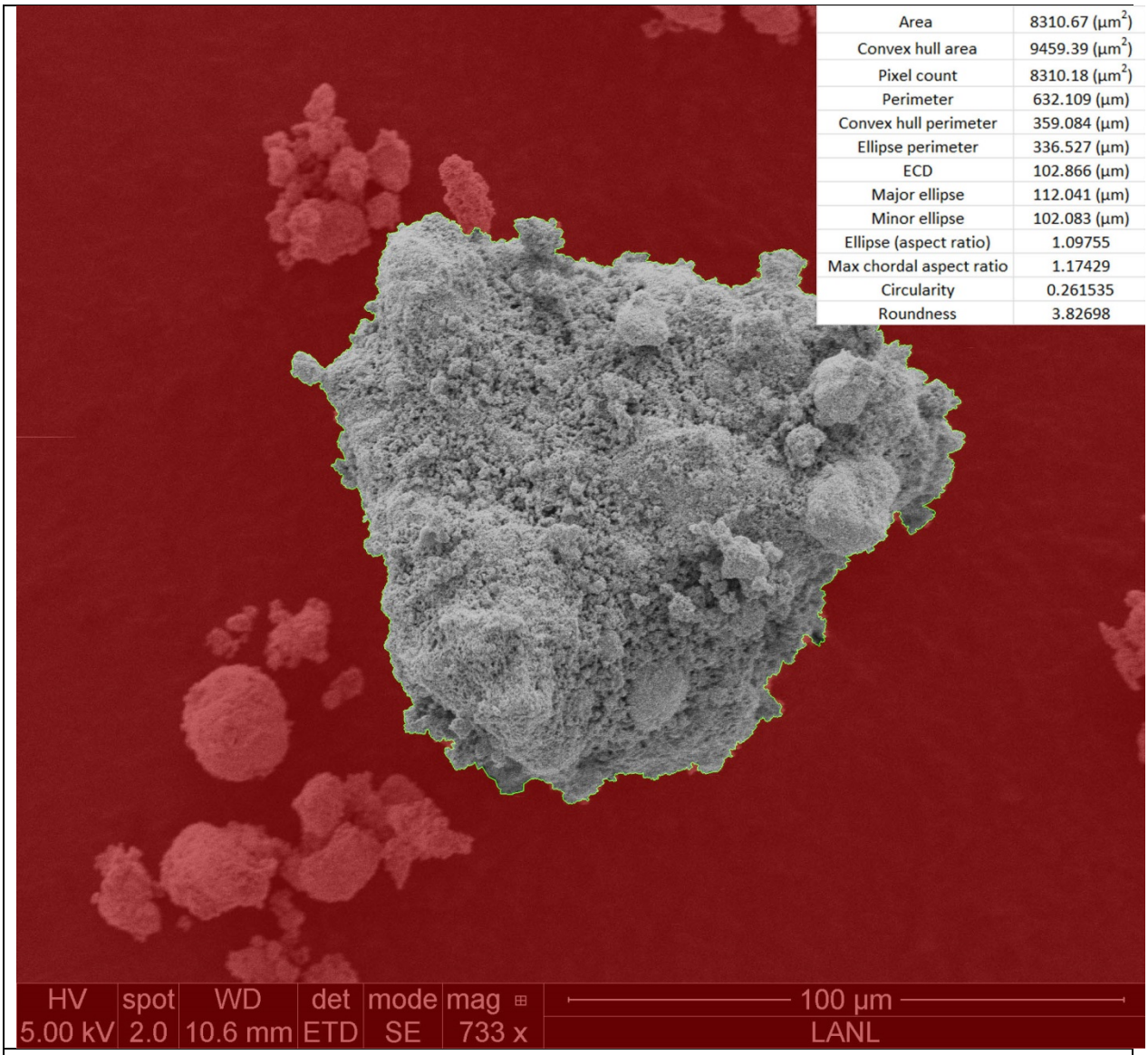

Figure 11. Large particle in Canada Key Lake ore, with morphological parameters calculated using MAMA.

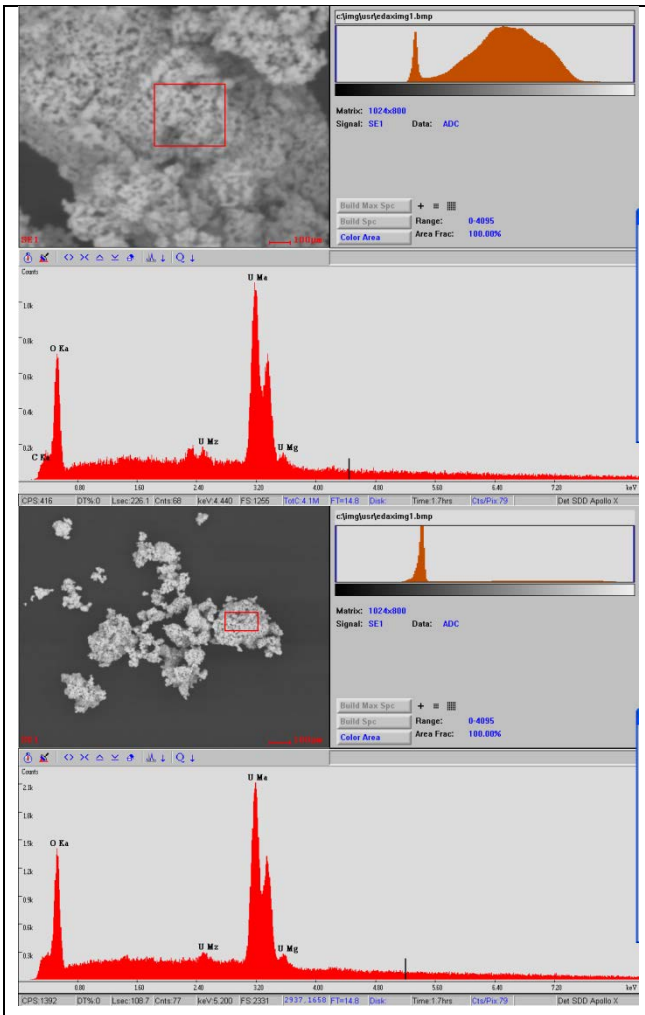

Figure 12. EDS spectra from representative CKL (left) and Namibia (right) particles.

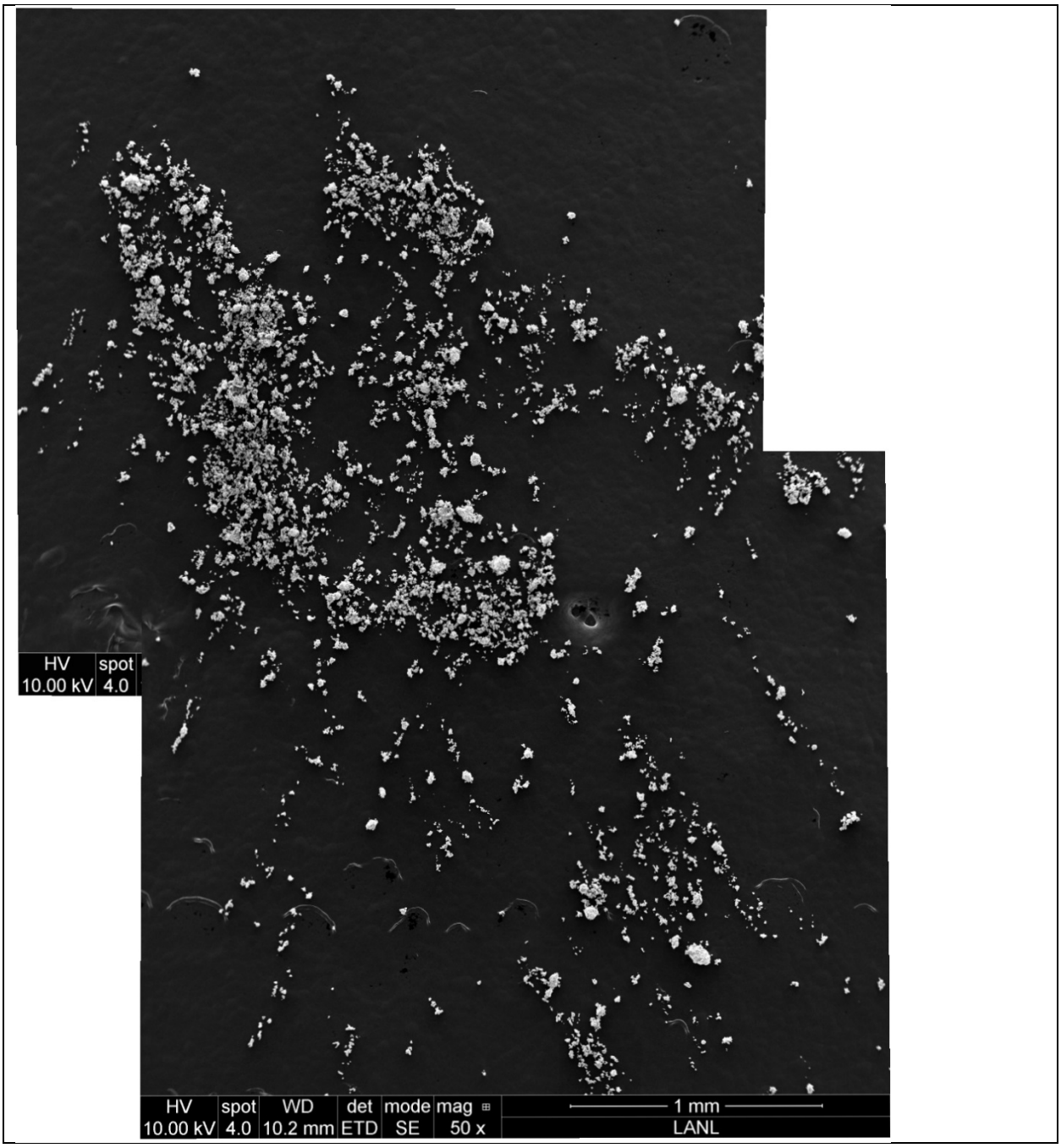
HV
10.00 kV
spot
4.0
HV
10.00 kV
spot
4.0
WD
10.2 mm
det
ETD
mode
SE
mag
50 x
1 mm
LANL

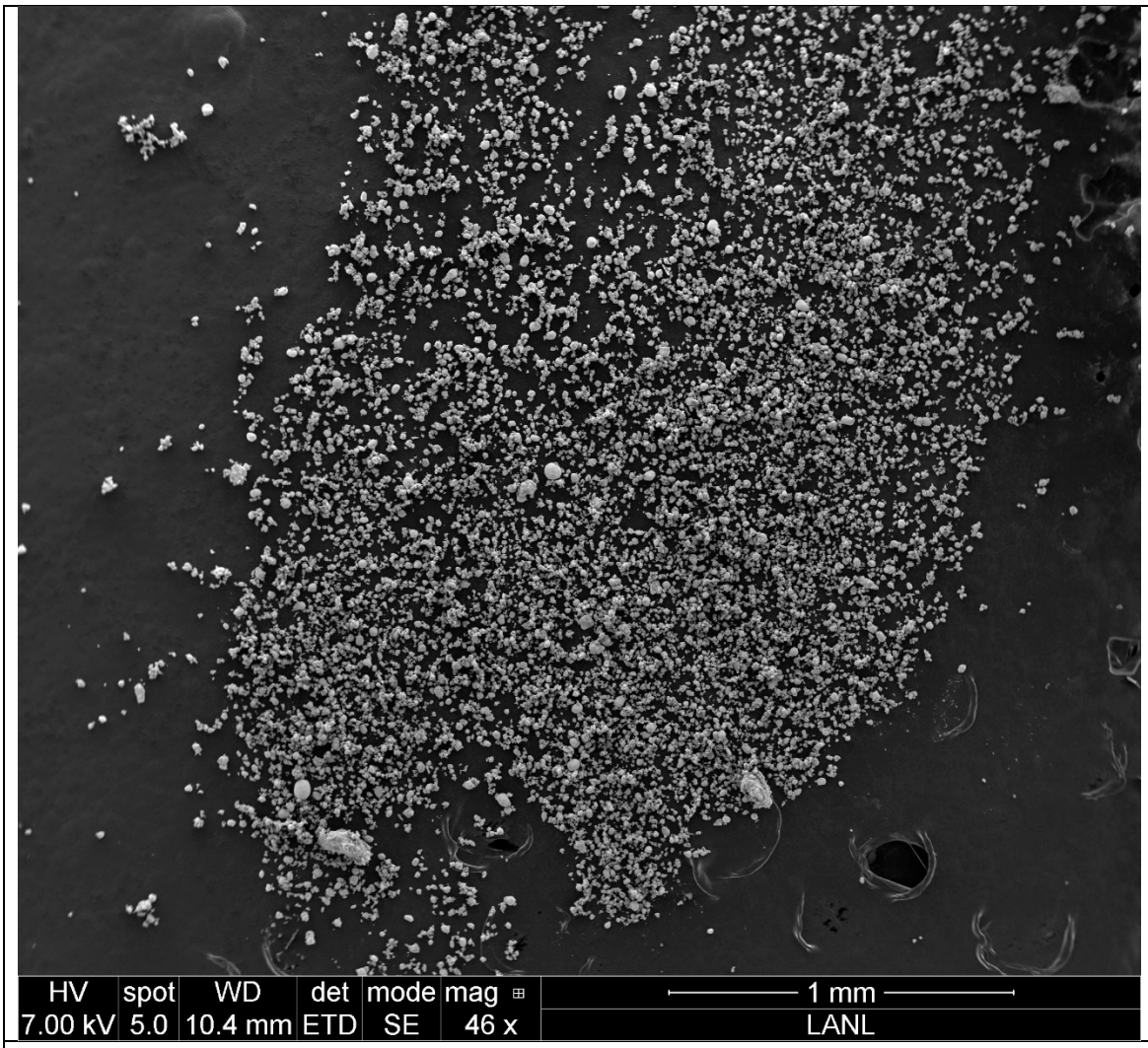

Figure 13. Micrographs of Namibia ore particles (above) and CKL ore particles (below) applied to tilted SEM stubs.

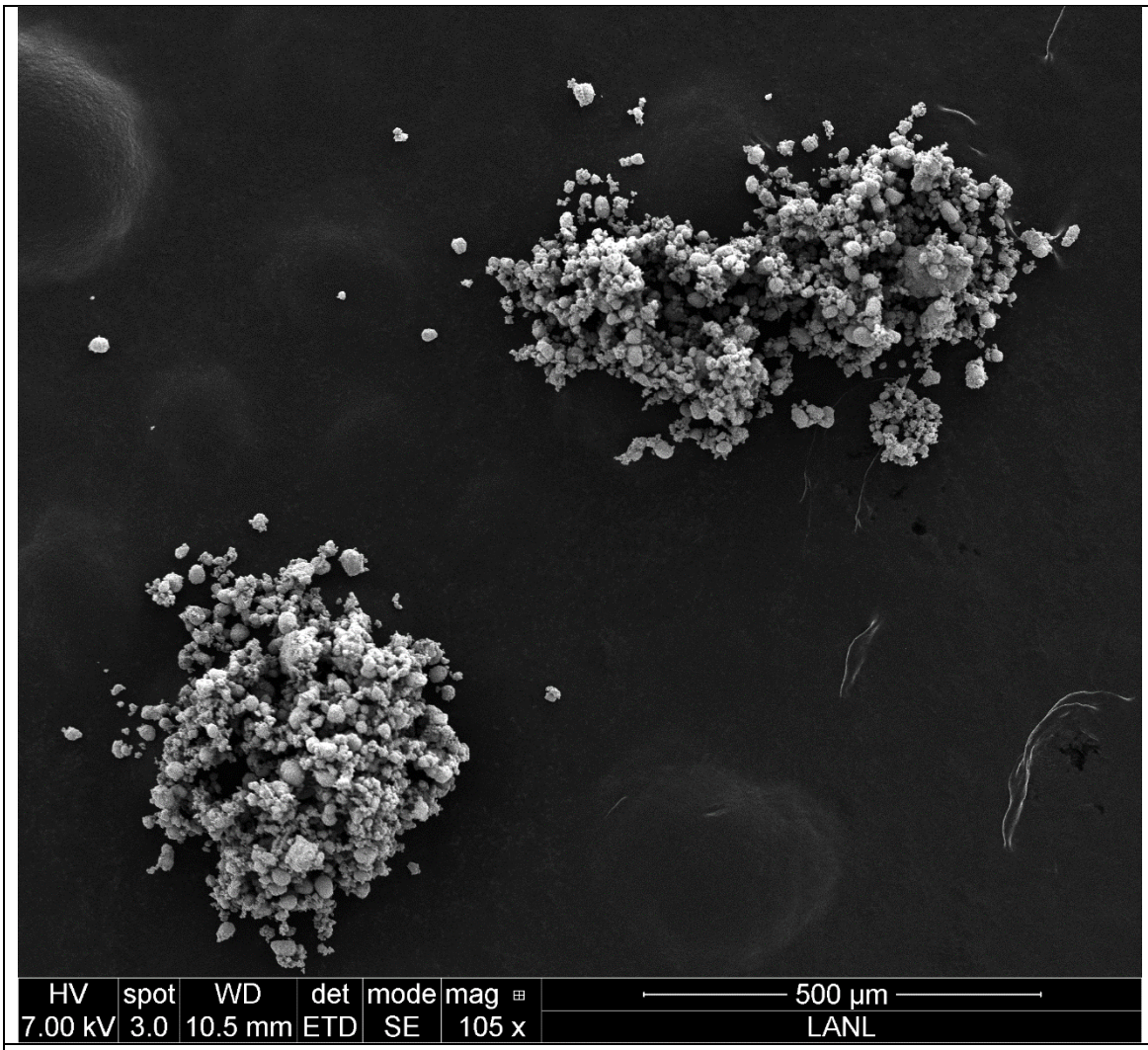

Figure 14. CKL particles applied using a foam-tipped swab to preserve large agglomerations.

Table 1. Statistical summary for CKL ore of all morphological parameters calculated by MAMA software (part 1).

CKL ore	*Area*	*Convex hull area*	*Pixel count*	*Perimeter*	*Convex hull perimeter*	*Ellipse perimeter*	*ECD*	*Major ellipse*
Mean	66.07	74.47	65.98	32.24	25.85	24.48	7.22	9.08
Standard Error	5.28	5.67	5.27	1.17	0.91	0.87	0.27	0.32
Median	25.22	29.15	25.07	25.28	20.51	19.41	5.66	7.56
Mode	1.66	22.23	1.66	17.47	#N/A	#N/A	#N/A	#N/A
Standard Deviation	112.28	120.60	112.23	24.99	19.38	18.50	5.66	6.75
Sample Variance	12605.68	14545.51	12594.52	624.49	375.56	342.17	32.05	45.59
Kurtosis	33.44	29.29	33.50	2.03	2.55	2.93	3.62	2.47
Skewness	4.70	4.36	4.71	1.28	1.34	1.40	1.54	1.32

Range	1096.81	1141.46	1096.79	150.23	121.95	118.28	37.13	42.96
Minimum	0.05	0.05	0.05	0.85	0.84	0.96	0.24	0.34
Maximum	1096.86	1141.51	1096.83	151.08	122.80	119.24	37.37	43.31
Sum	29928.13	33732.66	29890.97	14606.82	11711.80	11091.64	3270.52	4114.55
Count	453	453	453	453	453	453	453	453
Confidence Level(95.0%)	10.37	11.14	10.36	2.31	1.79	1.71	0.52	0.62

Table 2. Statistical summary for CKL ore of morphological parameters calculated by MAMA software (part 2).

CKL ore	*Minor ellipse*	*Ellipse*	*Max chordal*	*Circularity*	*Roundness*	*Perimeter convexity*	*Area convexity*	*GoEllipse*
Mean	6.34	1.52	1.48	0.52	2.10	0.83	0.86	1.28
Standard Error	0.24	0.02	0.02	0.01	0.07	0.00	0.00	0.01
Median	4.67	1.42	1.38	0.52	1.92	0.83	0.87	1.27
Mode	2.21	#N/A	2.00	#N/A	#N/A	#N/A	#N/A	#N/A
Standard Deviation	5.09	0.39	0.37	0.12	1.46	0.07	0.07	0.13
Sample Variance	25.92	0.15	0.14	0.01	2.14	0.00	0.00	0.02
Kurtosis	3.83	4.06	4.10	-0.55	341.63	-0.24	4.72	0.56
Skewness	1.60	1.72	1.71	0.06	17.28	-0.30	-1.44	0.63
Range	34.48	2.45	2.41	0.58	29.86	0.39	0.54	0.92
Minimum	0.24	1.01	1.01	0.24	1.22	0.59	0.42	0.89
Maximum	34.72	3.45	3.42	0.82	31.08	0.98	0.97	1.81
Sum	2872.51	686.85	668.19	237.37	951.71	375.36	390.35	581.71
Count	453	453	453	453	453	453	453	453
Confidence Level(95.0%)	0.47	0.04	0.03	0.01	0.14	0.01	0.01	0.01

Table 3. Statistical summary of morphological parameters for Namibia ore calculated by MAMA software (part 1).

Namibia ore	*Area*	*Convex hull area*	*Pixel count*	*Perimeter*	*Convex hull perimeter*	*Ellipse perimeter*	*ECD*	*Major ellipse*
Mean	32.03	38.83	32.00	24.00	18.52	17.37	5.00	6.53
Standard Error	3.15	3.86	3.14	0.87	0.60	0.56	0.16	0.21
Median	12.97	15.52	12.97	19.34	15.16	14.08	4.06	5.42
Mode	2.53	1.79	0.11	14.60	#N/A	#N/A	#N/A	10.53
Standard Deviation	77.24	94.88	77.22	21.43	14.84	13.83	3.98	5.23
Sample Variance	5966.39	9001.60	5963.15	459.14	220.31	191.19	15.82	27.36

Kurtosis	91.14	96.24	91.21	21.59	16.43	16.72	15.55	17.45
Skewness	8.48	8.68	8.48	3.45	3.03	3.05	2.98	3.05
Range	1016.98	1343.42	1016.84	229.66	141.88	133.65	35.62	53.95
Minimum	0.11	0.12	0.11	1.33	1.28	1.28	0.37	0.45
Maximum	1017.09	1343.54	1016.95	231.00	143.16	134.93	35.99	54.40
Sum	19313.95	23417.19	19297.77	14473.22	11170.19	10472.35	3013.23	3937.73
Count	603	603	603	603	603	603	603	603
Confidence Level (95.0%)	6.18	7.59	6.18	1.71	1.19	1.11	0.32	0.42

Table 4. Statistical summary for Namibia ore of morphological parameters calculated by MAMA software (part 2).

Namibia ore	*Minor ellipse*	*Ellipse*	*Max chordal*	*Circularity*	*Roundness*	*Perimeter convexity*	*Area convexity*	*GoEllipse*
Mean	4.39	1.52	1.47	0.49	2.18	0.82	0.84	1.32
Standard Error	0.15	0.01	0.01	0.01	0.03	0.00	0.00	0.01
Median	3.58	1.45	1.42	0.49	2.05	0.82	0.85	1.30
Mode	#N/A	1.46	1.50	#N/A	#N/A	0.74	0.85	#N/A
Standard Deviation	3.58	0.35	0.32	0.13	0.66	0.08	0.06	0.16
Sample Variance	12.84	0.12	0.10	0.02	0.43	0.01	0.00	0.03
Kurtosis	16.72	2.50	3.13	-0.47	3.13	-0.47	1.04	0.34
Skewness	3.12	1.33	1.43	0.11	1.44	-0.29	-0.81	0.65
Range	33.28	2.30	2.26	0.65	4.68	0.40	0.42	0.97
Minimum	0.32	1.02	1.01	0.17	1.22	0.58	0.55	0.95
Maximum	33.60	3.31	3.27	0.82	5.89	0.99	0.97	1.91
Sum	2648.41	916.03	887.26	298.26	1316.90	491.70	506.83	794.03
Count	603	603	603	603	603	603	603	603
Confidence Level (95.0%)	0.29	0.03	0.03	0.01	0.05	0.01	0.00	0.01

Table 5. Statistical parameters for ECD, for each ore type.

Equivalent Circular Diameter		
	Namibia	*CKL*
Mean (µm)	5.00	7.22
Standard Error	0.16	0.27
Median	4.06	5.66
Standard Deviation	3.98	5.66

Kurtosis	15.55	3.62
Skewness	2.98	1.54
Count	603	453
Confidence Level (95.0%)	0.32	0.52

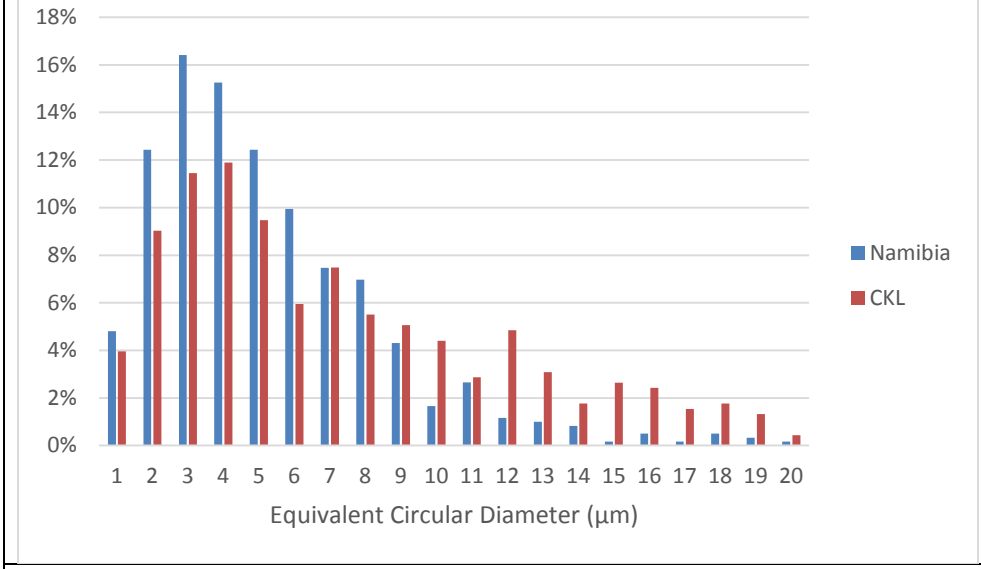

Figure 15. Histogram comparison of ECD for the two ore types.

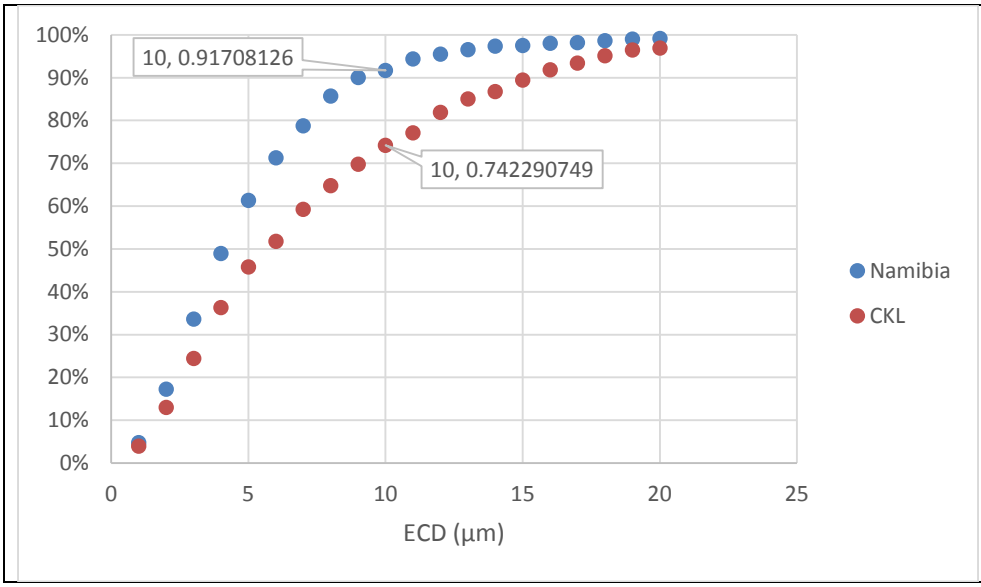

Figure 16. Cumulative distribution plot for ECD, showing measurably smaller particle diameter for the Namibia ore.

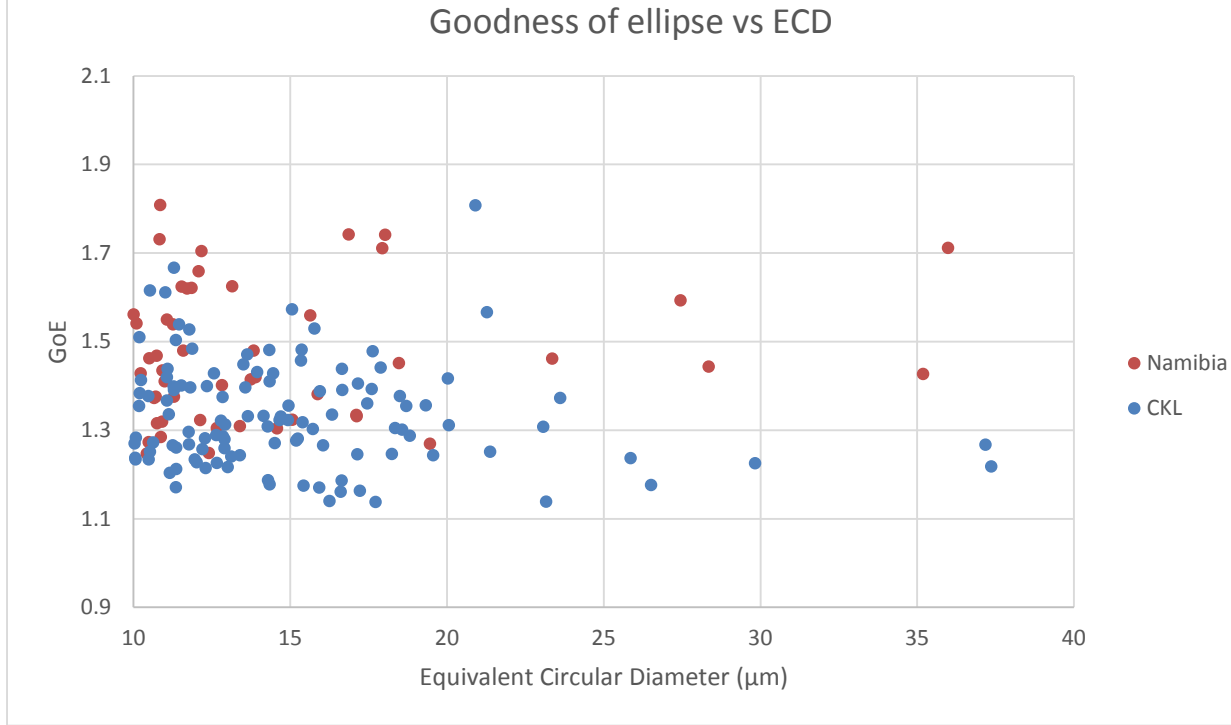

Figure 17. "Goodness of ellipse" parameter as a function of ECD for the two ore sources.